CFD SIMULATION OF A BURNER FOR SYNGAS CHARACTERIZATION: PRELIMINARY RESULTS AND EXPERIMENTAL VALIDATION

M. D'Amico*, U. Desideri** and F. Fantozzi**
*Biomass Research Centre – University of Perugia
**Department of Industrial Engineering – University of Perugia
Via Duranti, 06100 Perugia Italy

ABSTRACT: Biomass and Waste are distributed and renewable energy sources that may contribute effectively to sustainability if used on a small and micro scale. This requires the transformation through efficient technologies (gasification, pyrolysis and anaerobic digestion) into a suitable gaseous fuel to use in small internal combustion engines and gas turbines. The characterization of biomass derived syngases during combustion is therefore a key issue to improve the performance of small scale integrated plants because synthesis gas shows significant differences whith respect to Natural Gas (mixture of gases, low Calorific Value, hydrogen content, tar and particulate content) that may turn into ignition problems, combustion instabilities, difficulties in emission control and fouling. To this aim a burner for syngas combustion and LHV measurement through mass and energy balance was realized and connected to a rotary-kiln laboratory scale pyrolyzer at the Department of Industrial Engineering of the University of Perugia. A computational fluid dynamics (CFD) simulation of the burner was carried out to consider thermal inertias and heat transfer constraints and to investigate temperature and pressure distribution, and distribution of the combustion products and by products. The simulation was carried out using the CFD program Star-CCM+. Before the simulation a geometrical model of the burner was built and the volume of model was subdivided in cells. A sensibility analysis on the number of cells was carried out to estimate the approximation degree of the model. The model was validated with experimental data on propane combustion and the comparison between numerical results and experimental data provided useful information for following activities. The paper shows main results obtained during simulation with biomass pyrolysis syngas combustion in terms of heat transfer, emissions and heating value calculation. Preliminary comparison to selected experimental results are also provided.
Keywords: pyrolysis, syngas, analysis, low calorific value

1 INTRODUCTION

Residual energy sources such as biomass and waste may contribute effectively to meeting the Kyoto Protocol targets by reducing the use of fossil fuels. The current available technologies for the exploitation of biomass energy and waste are based on combustion and heat recovery in steam plants whose minimum size is economically suitable to the order of 5 MWe; the production of electricity on a small size (<1 MWe), though presents fewer problems in terms of accessibility and authorization, it is almost exclusively monopoly of internal combustion engines and microturbines, hence the need to convert biomass into a fuel, liquid or gaseous, suitable to be used on these engines. To this aim the University of Perugia has developed the integrated Pyrolysis recuperated plant IPRP technology [1-4] which allows B&W energy conversion on microscale in order to achieve sustainability for small communities.

A pilot IPRP plant was designed and built, at the Terni facility of the University of Perugia, with the help of data provided by a laboratory scale, electrically heated, rotary kiln.

1.1 Pyrolysis process

Pyrolysis is a solid thermal degradation at high temperatures (400 - 1100 ° C) in absence of an oxidizing agent or in presence of a limited amount that will not cause gasification. From an environmental perspective pyrolysis offers great attractions with the ability to degrade thermally wide variety of materials into solid gaseous and liquid fuels that may be used in internal combustion cycles, producing low emissions of oxides of nitrogen and sulfur. Compared to more current technologies such as incinerators, pyrolysis may provide higher energy recovery [5]. The products of pyrolysis reactions can be divided into three main components:

- Syngas: mainly composed of hydrogen, carbon oxides (CO, CO_2) and gaseous hydrocarbons such as methane, with a calorific value between 5-20 MJ/kg.
- Tar: is a condensable organic compound (bio-oil) characterized by a complex chemical composition: carboxylic acids, aldehydes, alcohols, water and tar vapors.
- Char: is a carbon residue characterized by a low ash content and a PCI relatively high (30 MJ/kg); it can be used as fuel to power the pyrolysis process or for drying biomass [6].

Although the three phases are present as a result of the pyrolysis process, it is possible to increase the yield of one of them, properly selecting the process conditions such as:

- the final temperature of reaction;
- the heating rate of biomass;
- the residence time of material;
- the size and physical form of biomass;
- the presence of certain catalysts.

Pyrolysis process can be divided in different phases depending on the temperatures reached by products [7]:

- for temperature values below 200°C producted only not combustible gas, mainly water vapor, small concentrations of CO_2, acetic and formic acid are;
- from 200°C to 280°C starts the devolatilization of some components of biomass that react together to form CO and some intermediate species such as oxygenated liquid hydrocarbons (alcohols) and acids;

- from 280°C to 500°C the exothermic reactions of the second stage cause a rise of temperature and lead to the formation of combustible gases (CO, CH_4 and H_2) and flammable liquid products in form of tar;
- above 500°C, the initial biomass is almost totally degraded and the reactions of the second stage are prevalent than the first.

Studies [8] show that for almost all types of biomass maximum liquid yields are obtained between 475-525 °C if the residence time of volatile components is between 0.2-0.6 s. Moreover higher temperatures increase the yield of syngas and also changes its chemical composition: the percentage of hydrogen and carbon monoxide increases while methane is decreasing, so the final result is a lower heating value.

1.2 The laboratory pyrolyzer: test bench layout

Biomass is loaded into a hopper and fed continuously into the rotary kiln through a screw conveyor driven by an electric motor. The rotary kiln is made of an AISI 304 steel pipe provided with ceramic external heaters to bring the reactor to the temperature necessary to reach pyrolysis. The heat needed for pyrolysis is supplied electrically through two shells in ceramic. Pyrolysis process products move through natural motion to the discharge section, at the end of pyrolyzer, the gaseous phase (tar and gas) is expelled from the top while the solid phase (char) is discharged by gravity. Char is collected in a tank while the gaseous phase passes through a cleaning section: namely a calm chamber, for dust removal and char deposit, and a humid quencher-scrubber, made of a cylinder full of water through which the gas gurgles, condensing water and tar vapors [9,10].

The cooled gas is sucked by a blower before which there is a filter system to prevent the entrance of water and tar residues in the machine. Cleaned and cooled gas is burned in a combustion chamber, the flame is continuously ignited by a natural gas pilot flame. To monitor the combustion flue gases a portable analyzer Lancome III is used, placing the sampling probe at the exit section of the exhaust fumes.

2 OBJECTIVE OF THE WORK

The aim of the research is to study low btu gas combustion, especially syngas from pyrolysis, by coupling biomass experimental data from an adiabatic burner and a CFD model of the burner itself. Results obtained from experimental tests of known gas combustion are used to determine the heat losses of the combustion chamber. The CFD model fused with experimental data, will heating value and emission of pollutants of any fuel mixture. A CFD reference run to check the numerical results with those obtained from the experimental combustion of propane.

3 CONSTRUCTION OF THE CFD MODEL

3.1 The combustion chamber

The burner, installed on the gas line, is medium speed, type “nozzle mix”, whose constructive characteristics allows to work in a stable flame with air excess of 800%. The use of an excess air burner is performed by maintaining constant volume of fuel gas with a modulating valve placed on the fuel pipe and with constant air input. The burner has a pilot flame always on, to ensure the ignition of gas-air mixture where the composition is within the limits of flammability, separately fed with methane (pressure of 50 mbar) and with a power of about 2.3 kW, the pilot flame is an independent burner complete of ignition electrode and flame detection. The burner works in excess of air provided by a centrifugal fan with medium pressure with exhaust gas temperature control. Figure 1 shows a picture of the combustion chamber. Thermocouples were positioned in various points of the burner outer surface to monitor the increase of temperature due to heat flow.

Figure 1: Combustion chamber

3.2 Geometrical model and mesh grid

One computational domain was realized reproducing the real geometry of the CC. In Figure 2 the computational domain is shown.

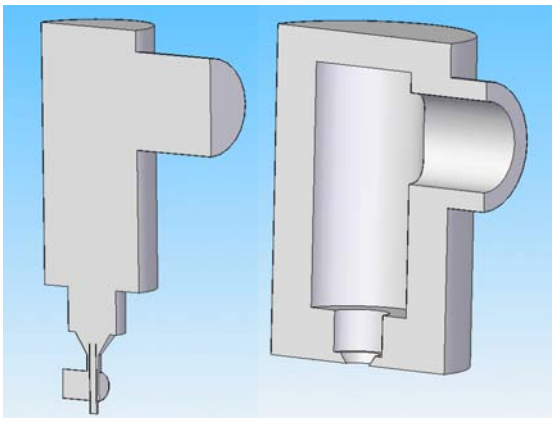

Figure 2: Geometrical model of CC

The numerical simulations were carried out with the commercial CFD code STAR CCM+ produced by CD-ADAPCO [11]. The physical model considered is a 3D, multi component ideal gas, standard K-ε turbulence

model, reacting, non-premixed combustion. For the numerical analysis, a 180 degree sector of the CC is used, due to burner symmetry. The volume grids used in numerical analysis are generated with STAR CCM+.

Regarding the size of the cells was considered the reference value of 1.5 cm for the fluid region, while the area bounded by the control cylinder was chosen to reduce this value to 25% (0.375 cm). For the solid region, affected by phenomena much less complex and sensitive, was considered a higher value as a reference dimension (2.5 cm). The model considers polyhedral mesh: 374,882 cells in fluid region and 15,492 cells in solid region.

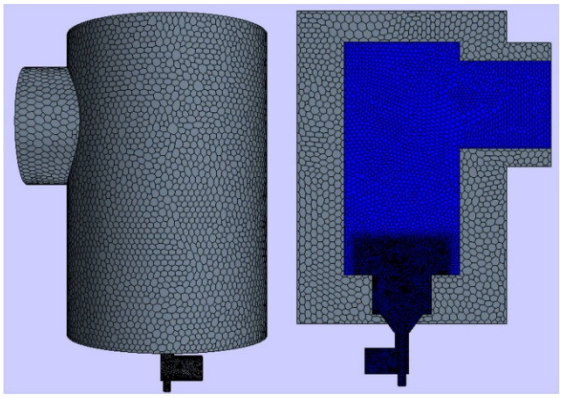

Figure 3: Combustion chamber: mesh grid

3.3 Turbulence and combustion model

The turbulence model used is the Standard K-Epsilon turbulence model. This is a two-equation model in which transport equations are solved for the turbulent kinetic energy and its dissipation rate. The transport equations are in the form suggested by Jones and Launder [12], with coefficients suggested by Launder and Sharma [13]. Some additional terms have been added to the model in STAR-CCM+ to take into account other effects such as buoyancy and compressibility. The turbulence parameters have been introduced through the value of Turbulent Intensity *I* and the Length Scales *L* using eq.:

$$k = \frac{3}{2}(Iv)^2$$

$$\varepsilon = \frac{C_\mu^{3/4} k^{3/2}}{L}$$

The value of *I* and *L* used in the numerical analysis are shown in Table I:

Table I: Turbulent intensity and length scale

Turbulent Intensity I	Length Scales L
0.1	0.1 x Hydraulic diameter

For the analyses, a Hybrid Kinetics/Eddy Breack-up (EBU) combustion model was used. In this model the reaction rate *Ri* is equal to the minimum value between the standard EBU and the kinetics model. In the standard EBU model individual species in the global reaction are assumed to be transported at different rates according to their own governing equations.

3.4 Chemical scheme and boundary conditions

For the numerical analysis of propane combustion a chemistry model involving 5 chemical species in 2-steps reactions was considered. The reactions, the value of the pre-exponential factor, temperature exponent and activation energy for each reaction and the exponent rate for each species [14] are reported below:

$$C_3H_8 + \frac{7}{2}O_2 \rightarrow 3CO + 4H_2O$$

$$CO + \frac{1}{2}O_2 \leftrightarrow CO_2$$

$$R_1 = 5.62\times10^9 \times e^{-\frac{1.256\times10^8}{RT}} [C_3H_8]^{0.1}[O_2]^{1.65}$$

$$R_2 = 2.239\times10^{12} \times e^{-\frac{1.710^8}{RT}} [CO][O_2]^{0.25}[H_2O]^{0.5}$$

Table II shows the data about mass flow rate and temperature, both for fuel and air, derived from previous experimental tests and then used as input values and boundary conditions in the simulations.

Table II: Mass flow rate and temperature of fuel and air (propane)

INLET	AIR	FUEL
Mass flow rate (kg/s) [x 2]	0.046575 [0.093150]	0.001010 [0.002020]
Temperature (K)	288	288

For the numerical analysis of syngas combustion a chemistry model involving 6 chemical species in 3-steps reactions was considered.

The reactions, the value of the pre-exponential factor, temperature exponent and activation energy for each reaction and the exponent rate for each species [15,16] are reported below:

$$CH_4 + \frac{3}{2}O_2 \rightarrow CO + 2H_2O$$

$$CO + \frac{1}{2}O_2 \rightarrow CO_2$$

$$H_2 + \frac{1}{2}O_2 \rightarrow H_2O$$

$$R_1 = 5.012\times10^{11} \times e^{-\frac{2\times10^8}{RT}} [CH_4]^{0.7}[O_2]^{0.8}$$

$$R_2 = 2.239\times10^{12} \times e^{-\frac{1.7\times10^8}{RT}} [CO][O_2]^{0.25}[H_2O]^{0.5}$$

$$R_3 = 9.870\times10^8 \times e^{-\frac{3.1\times10^7}{RT}} [H_2][O_2]$$

Table III shows the data about mass flow rate and temperature, both for fuel and air, derived from previous experimental tests and then used as input values and boundary conditions in the simulations.

Table III: Mass flow rate and temperature of fuel and air (syngas)

INLET	AIR	FUEL
Mass flow rate (kg/s) [x 2]	0.023065 [0.046130]	9.014E-4 [0.001803]
Temperature (K)	288	288

For the physical definition of the solid model was set a 3D, stationary and constant density model. The properties of the insulating layer are shown in Table IV.

Table IV: Properties of the insulating layer

BRICK (Insulating Layer)	
Temperature (K)	288
Density (kg/m^3)	1400
Specific Heat (J/kg K)	920
Thermal conductivity (W/m K)	0.4

The initial composition of the syngas (illustrated in Table V), was considered assuming data from a chromatograph analysis of the samples taken during the pyrolisis test.

Table V: Syngas composition from Pyrolysis test

SPECIE	MASS FRACTION
CH_4	0.0214
CO	0.1661
CO_2	0.2786
H_2	0.0009
N_2	0.4345
O_2	0.0985

In both stationary simulations an external condition was applied to the insulating layer in terms of wall temperature (thermal specification) considering the temperature detected at the end of the experimental tests with appropriate thermocouples positioned in different locations of the external layer of combustion chamber; the temperature values mentioned and used in numerical simulations were 327 K for the case of propane nd 288 K for the case of syngas.

The simulations at transient conditions are aimed to a partial comparison of the test data: the need to work with very low time-step, (on the order of 10E-5 - 10E-3 sec), and the consequent duration of a simulation process have suggested a comparison of data referred to a time-step not to far from the start of the experimental test.

4 RESULTS AND DISCUSSION

The test of the combustion chamber was made for the propane case and syngas case, with a constant mass flow rate of fuel and air. The numerical value of mass flow rate is referred to half section because of the symmetry of the burner. The simulations were validated in terms of emissions of pollutants and temperature.

4.1 Propane: numerical simulations

The calculated temperature distribution referred to steady state and to 60s transient are shown in Figure 4, 5, 6 and 7. Simulated propane burns with an elongated flame characterized by a tight combustion cone angle, which probably might be related to a fast mixing. Propane combustion leads to a pick temperature of about 2300 K with points of maximum temperature placed around the flame axis.

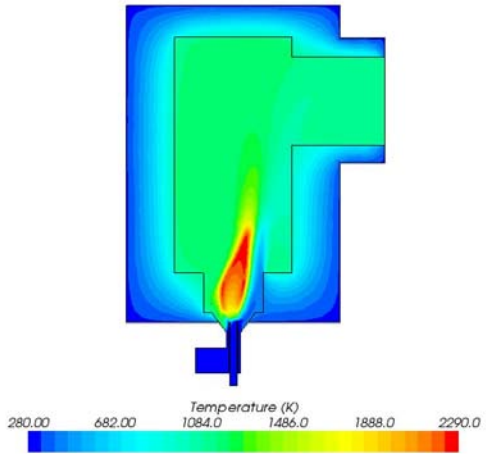

Figure 4: Temperature profile in plane x-z: steady state.

Regarding Figures 4, 5, 6 and 7 it is possible to see how the temperature could be comparable in terms of numerical values and distribution; according to experimental data detected with three thermocouples positioned on both sides and upper part of the burner, the temperature of insulating layer after a transient of 60 seconds remains constant and equal to 288 K because the propagation rate of heat is not sufficient to cross, in the considered time, the whole insulating layer.

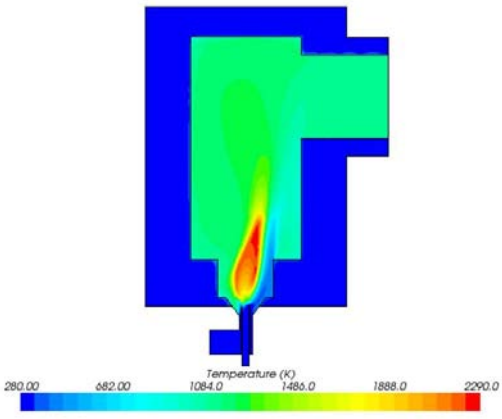

Figure 5: Temperature profile in plane x-z: transient of 60 seconds.

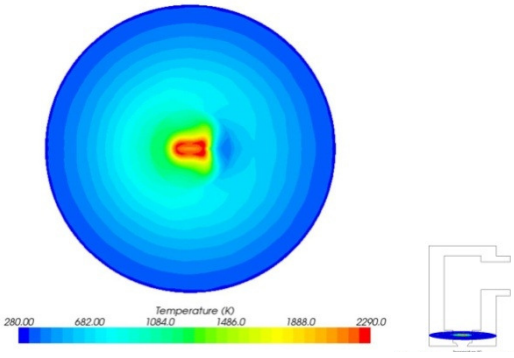

Figure 6: Temperature profile in plane x-y: steady state.

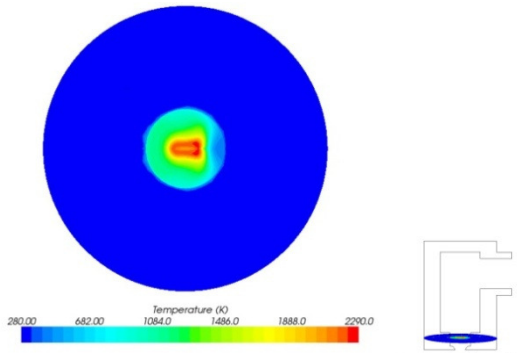

Figure 7: Temperature profile in plane x-y: transient of 60 seconds.

In Figure 8 and 9 is shown temperature profile in the outlet section of the burner. The highest temperature of about 1200 K is, also in this case, placed around the symmetry axis. Distribution still shows after transient of 60 seconds significant differences.

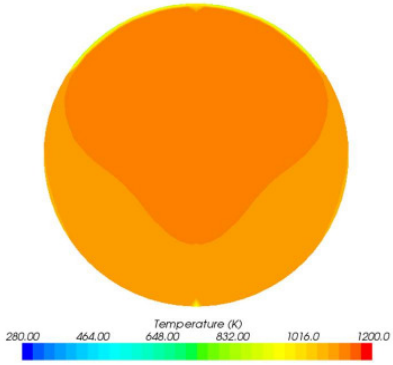

Figure 8: Temperature profile in outlet section: steady state.

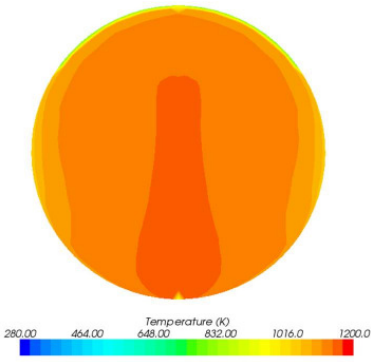

Figure 9: Temperature profile in outlet section: transient of 60 seconds.

Figure 10 compares the transient temperature profilein the outlet section obtained numerically and experimentally; the difference in terms of temperature between numerical and experimental data can be attributed to:

- different positioning of the thermocouple for recording data of temperature;
- absence of Radiation in the CFD model used.

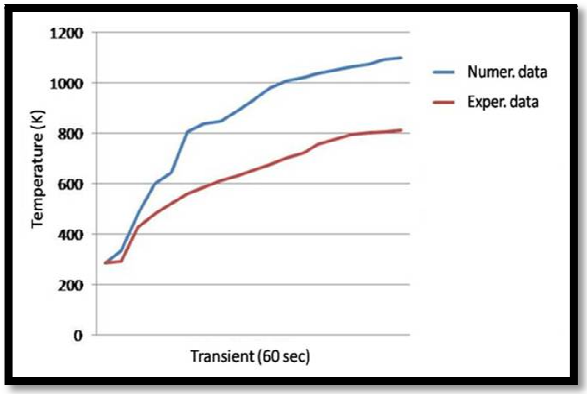

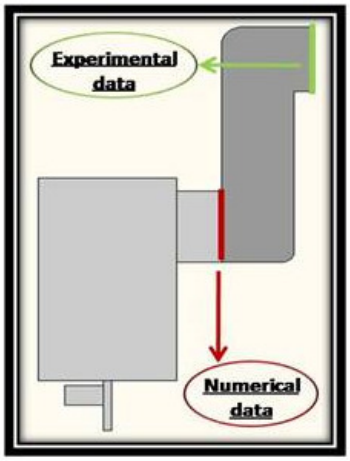

Figure 10: Temperature profile in the outlet section: transient of 60 seconds.

Emission measurement results are summarized in Table VI, where concentration values are referred on a dry basis.

Carbon monoxide concentration is very low both in experimental and numerical conditions: the differences between experimental and numerical values are probably due to the combustion model used that does not consider the third step reaction meaning the dissociation of CO_2 in CO and O_2. The version of the CFD software used for the transient case still had no the mechanism for determining Zeldovich NO_x.

Emissions measurements however are very close to the base scale (zero) of the instrument and therefore affected by an error not quantificable.

Table VI: Emission measurements: steady state.

Specie emission	Experimental Data	Numerical Data
O_2 (% vol)	14,30	14,35
CO (ppm)	41,00	4,00
CO_2 (% vol)	4,60	4,35
NOx (ppm)	19,00	12,00

Table VII: Emission measurements: transient of 60 seconds.

Specie emission	Experimental Data	Numerical Data
O_2 (% vol)	12,01	13,32
CO (ppm)	23,00	11,00
CO_2 (% vol)	4,58	5,02

Figure 11 shows the energetic efficiency of the combustion chamber during the experimental test (transient of 70 minutes); this performance confirms that the burner is not adiabatic.

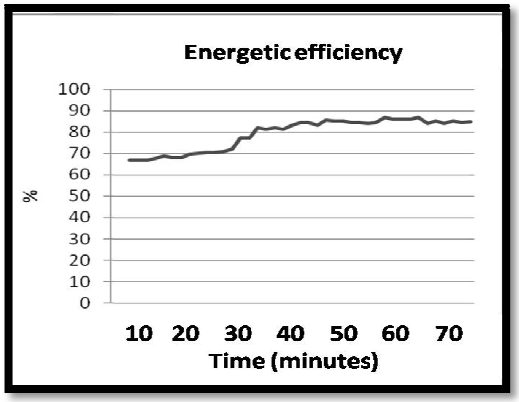

Figure 11: Energetic efficiency of combustion chamber during the experimental test.

4.2 Syngas: numerical simulations

The calculated temperature distribution referred to steady state and to a transient of 20 seconds, are shown in Figure 12, 13, 14 and 15; the combustion of syngas reaches a maximum temperature of around 750 K with peaks, also in this case, positioned around the flame axis.

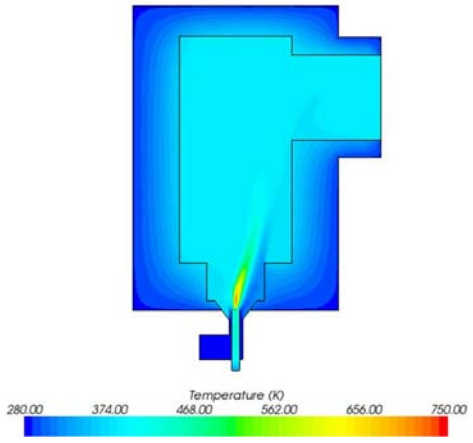

Figure 12: Temperature profile in plane x-z: steady state.

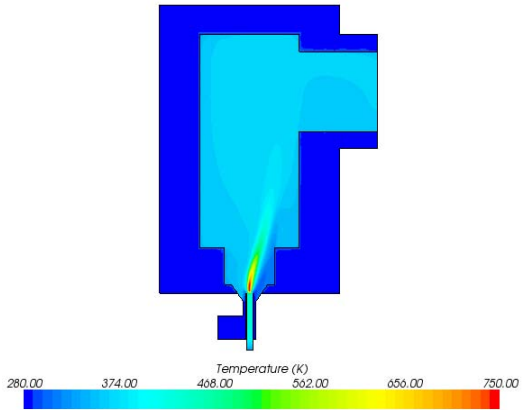

Figure 13: Temperature profile in plane x-z: transient of 20 seconds.

Regarding Figures 12, 13, 14 and 15 it is possible to see, also in this case, how the temperature could be comparable in terms of numerical values and distribution; according to experimental data.

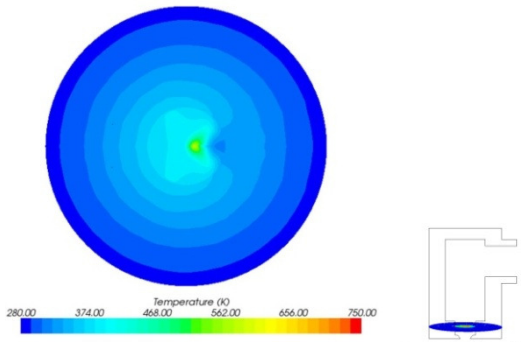

Figure 14: Temperature profile in plane x-y: steady state.

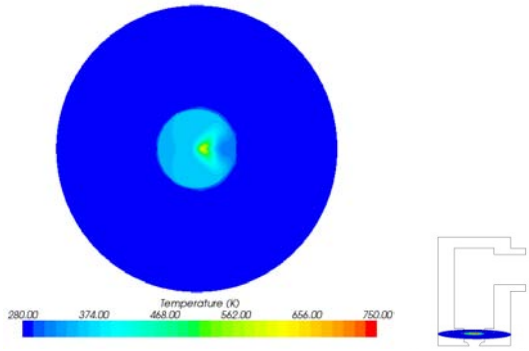

Figure 15: Temperature profile in plane x-y: transient of 20 seconds.

In Figure 16 and 17 is shown temperature profile in the outlet section of the burner. The highest temperature of about 390 K is, also in this case, placed around the symmetry axis. Distribution still shows after transient of 20 seconds significant differences.

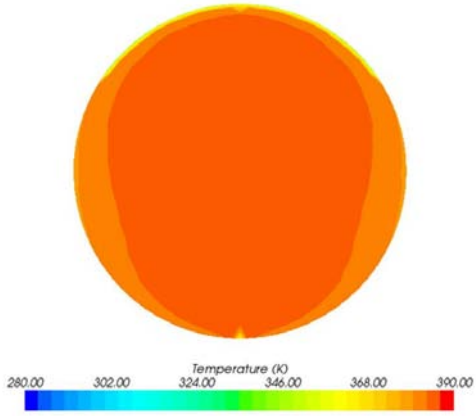

Figure 16: Temperature profile in outlet section: steady state.

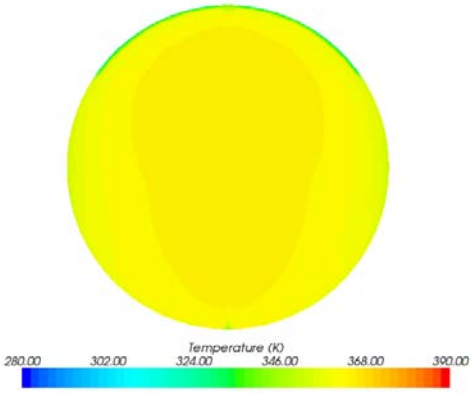

Figure 17: Temperature profile in outlet section: transient of 20 seconds.

Emission measurement results are summarized in Table VIII and IX.

The data about NOx emissions, referred to the steady state, can be attributed to the low temperatures reached during the combustion; comparing data of carbon monoxide concentration referred to the transient and steady state it is possible to see how these values are characterized by an initial peak that decreases, with increasing of temperature, due to the mechanism of oxidation.

The version of the CFD software used for the transient case still had no the mechanism for determining Zeldovich NO_x

Table VIII: Emission measurements: steady state.

Specie emission	Experimental Data	Numerical Data
O_2 (% vol)	20,65	20,00
CO (ppm)	130,00	120,00
NOx (ppm)	0,12	0,00

Table IX: Emission measurements: transient of 20 seconds.

Specie emission	Experimental Data	Numerical Data
O_2 (% vol)	20,46	20,21
CO (ppm)	1225,72	1366,76

Figure 18 compares the transient temperature profile in the outlet section obtained numerically and experimentally; the difference in terms of temperature is attributable, also in this case, to:

- different positioning of the thermocouple for recording data of temperature;
- absence of Radiation in the CFD model used.

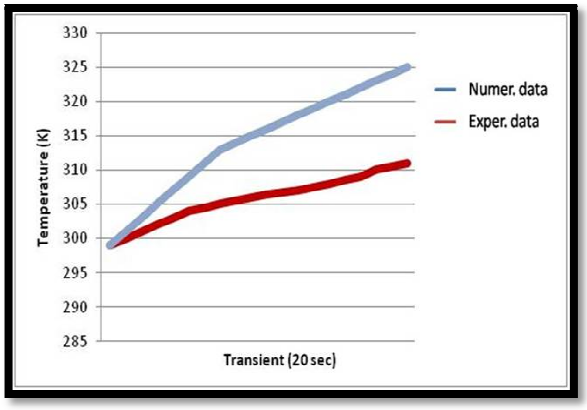

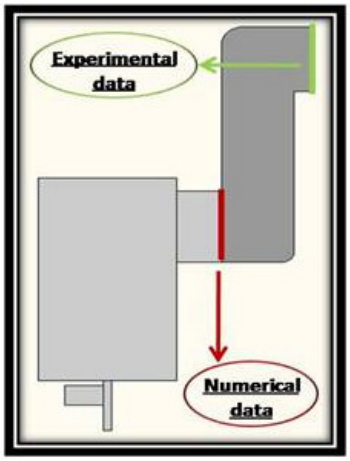

Figure 18: Temperature profile in outlet section: transient of 20 seconds.

Figure 19 shows the energetic efficiency of the combustion chamber during the experimental test (transient of 5 minutes); this performance confirms that the burner is not adiabatic.

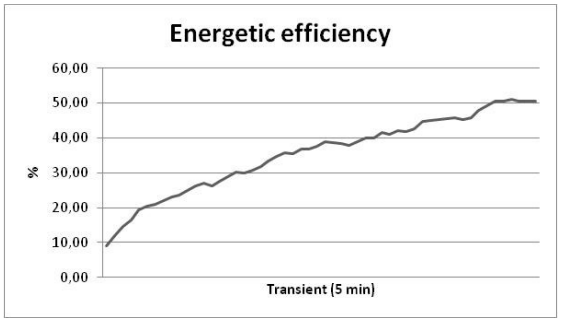

Figure 19: Energy efficiency of combustion chamber during the experimental test.

5 CONCLUSIONS

This work presents the preliminary results reached comparing experimental results obtained fuelling a quasi adiabatic combustor with a gas of known lower heating value (propane) and numerical results obtained simulating the same combustion with CFD software in order to compare emissions of pollutants and the distribution of temperature in the most interesting areas of the burner.

The CFD model built, having validated the experimental results, was subsequently implemented and used to construct a second model for the combustion of syngas.

The results obtained in terms of emissions and distribution of temperature were compared with those derived from experimental combustion of syngas produced with the pyrolysis;

Results show that it was constructed in this way a fluid-dynamic model of the combustion chamber in order to determine, only using the CFD model, the values, as close to reality, of the lower heating value and emissions of pollutants of any syngas produced with pyrolysis.

6 NOMENCLATURE

CC	Combustion Chamber
CFD	Computational Fluid Dynamics
IPRP	Integrated Pyrolysis Regenerated Plant
I	Turbulent Intensity
L	Length Scale
k	Turbulent Kinetic Energy
ε	Dissipation Rate
LHV	Lower Heating Value
μ	Dynamic Viscosity
ν	Kinematic Viscosity
C	Constant
EBU	Eddy Break-Up
R	Arrhenius rate of reaction

7 REFERENCES

[1] Fantozzi F., D'Alessandro B., Desideri U. (2005). IPRP – Integrated Pyrolysis Recuperated Plant – An efficient and scalable concept for gas turbine based energy conversion from biomass and waste. Journal of engineering for gas turbines and power, vol. 127; p. 348-357, ISSN: 0742-4795.

[2] Fantozzi F., D'Alessandro B., Bidini G. (2003). IPRP – Integrated Pyrolysis Regenerated Plant – Gas Turbine and externally heated Rotary Kiln as a biomass and waste to energy conversion system. Influence of thermodynamic parameters. Proceedings of the institution of mechanical engineers. Part A, Journal of power and energy, vol. 217; p. 519-527, ISSN: 0957-6509.

[3] Bidini G., Desideri U., Fantozzi F. (2003). Distributed generation of electricity from biomass using pyrolysis technology. Wood Energy, vol. 1; p. 35-37, ISSN: 1811-2722.

[4] Fantozzi F., D'Alessandro B., Desideri U. (2007). An IPRP (Integrated Pyrolysis Recuperated Plant) microscale demonstrative unit in central Italy. In: ASME Turbo Expo 2007: Power for Land, Sea and Air. Montreal, Canada, 14-17 Maggio 2007.

[5] Fortuna, F., Cornacchia, G., Mincarini, M., and Sharma, V.K., 1997, Pilot scale experimental pyrolysis plant: mechanical and operational aspects, Journal of Analitical and Applied Pyrolysis,. 403-417.

[6] Bridgwater, A.V., and Peacocke, G.V.C., 2000, Fast pyrolysis processes for biomass, Renewable and Sustainable Energy Reviews, 4, 1-7.

[7] Browne, F.L., 1958, Theories on the combustion of wood and its control, U.S. Forest Prod. Lab., Rep. 2136, p. 59, Madison, Wis.

[8] Scott, D.S., Majersky, P., Piskorz, J., and Radlein, D., 1999, A second look at fast pyrolysis of biomass - the RTI process, Journal of Analytical and Applied Pyrolysis, 23-37.

[9] Fantozzi F., Desideri U. (2004). Micro scale rotary kiln pyroliser for syngas and char production from biomass and waste – Reactor and test bench realization. In: ASME PAPER GT2004-54186.

[10]Fantozzi F., Desideri U., Bartocci P., and Colantoni S. (2006) Rotary kiln slow pyrolysis for syngas and char production from biomass and waste - Part 1 Working envelope of the reactor - ASME paper no. GT-2006-90818.

[11] Jones, W.P. and Lander, B.E. (1972). The prediction of laminarization, STAR CCM+ Version 4.02.007, User Guide, @2009 CD-adapco.

[12] Jones,W.P. and Lander, B.E. (1972). The Prediction of Laminarization with a Two-Equation Model of Turbulence, Int. J. Heat and Mass Transfer, vol. 15, pp. 301-314.

[13] Launder, B.E. and Sharma, B.I. (1974). Application of the Energy Dissipation Model of Turbulence to the Calculation of Flow Near a Spinning Disc, Letter in Heat and Mass Transfer, vol. 1, no. 2, pp 131-138.

[14] Calchetti G., Giacomazzi E., Rufoloni M., Giordano D. (2003) Simulazione di un transitorio di fiamma su un bruciatore sperimentale a propano. EHE 03/037, ENE-IMP, ENEA (in italian).

[15] Dryer F.L. and Glassman I., (1973). High temperature oxidation of CO and CH_4 ,14^{th} Symposium (int.) on combustion. The Combustion Institute, p. 987.

[16] Westbrook, C.K., Dryer, F.L. (1981). Simplified reaction mechanisms for the oxidation of hydrocarbon fuels in flames, Combustion Science and Technology, vol. 27, 31-43.

[17] D'Amico M. (2010). Simulazioni CFD e prove sperimentali della combustione di gas poveri in torcia, PhD thesis, University of Perugia (in italian).